Sławomir JODZIS, Tomasz SMOLIŃSKI, Piotr SÓWKA

Politechnika Warszawska, Wydział Chemiczny

Application of a concentric actuator for ozone synthesis under surface discharge conditions

Abstract. *The results of studies on the ozone synthesis under discharges generated on the surface of the ceramic actuator built as the concentric strips electrode system are presented. Experiments were carried out in pure oxygen, using the high voltage push-pull inverter. The ozonizer, in which the gas flows with variable linear velocity was used. The ozone concentrations and the process energy efficiency show the possibility of effective ozone generation in the reactors with non-conventionally organized discharge space. (**Zastosowanie koncentrycznego elementu wyładowczego do syntezy ozonu w wyładowaniach powierzchniowych**).*

Streszczenie. *Przedstawiono wyniki badań nad syntezą ozonu w wyładowaniach powierzchniowych, wytwarzanych na powierzchni ceramicznego elementu wyładowczego (actuatora). Elektroda wysokonapięciowa actuatora składała się z zespołu koncentrycznych ścieżek przewodzących. Eksperymenty prowadzono w czystym tlenie przy użyciu zasilacza typu push-pull. Używano ozonatora, przez który gaz płynął z wymuszaną, stale rosnącą prędkością liniową. Uzyskane stężenia ozonu oraz wydajności energetyczne procesu wskazują na możliwość efektywnego wytwarzania ozonu w reaktorach o niekonwencjonalnie zorganizowanej przestrzeni reakcyjnej.*

Keywords: ozone synthesis, surface discharges, ceramic actuator, concentric ozonizer.
Słowa kluczowe: synteza ozonu, wyładowania powierzchniowe, ceramiczny element wyładowczy, ozonator koncentryczny.

Introduction

The ozone synthesis process is typically carried out in dielectric barrier discharge (DBD) type ozonizers, in which the gas flows between the walls of the concentric tubes. The discharge system consists of electrodes, between which the layer of solid dielectric and the layer of the gaseous dielectric occur. The space filled with the gas (the discharge gap) has a form of a cylindrical capacitor C_g, which is intentionally broken. The discharge occurs, when the gas electric strength is exceeded, i.e. when the total supplying voltage on the capacitors connected in serial is suitably high (Fig. 1). The current is limited by the capacitive reactance of the solid dielectric C_d. The discharges generated in the gas have a volume character. They consist of numerous, dispersed microdischarge channels. From the electric point of view the discharge phenomenon in the gap are the losses, which are symbolized by the resistance R_g (Fig. 1). The DBD type ozonizer is a leading load with the high non-linear voltage-current characteristics, which appears when the gaseous gap is broken. In order to provide the uniform dispersion of the microdischarge channels in the discharge gap, the ozonizer construction must ensure a stable width of the discharge gap. Also the dielectric thickness should be uniform.

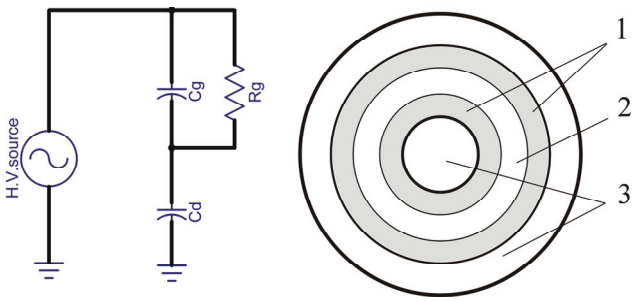

Fig.1. Equivalent circuit diagram of the DBD and typical tubular discharge system; Cg – gas capacity, Rg – resistance of a discharge gap, Cd – capacity of a solid dielectric, 1 – dielectric (Cd), 2 – discharge gap (Cg), 3 – cooling liquid

In the surface discharge (SD) systems the discharges presence is independent on the gas layer thickness in the electrode surrounding. The surface discharges can be obtained on the surfaces with the diversified shapes. Due to that the simplification of the ozonizer construction is possible. In order to generate surface discharges, simple discharge elements are usually applied, which are built of parallel strip electrodes [1-9], over which the gas flows. In this paper the results of studies on the application of an untypical discharge element, which was built of concentric circle electrodes located on a thin, flat ceramic support are presented. The gas flowed with the increasing linear velocity [10] to shorten the residence time of a concentrated ozone, when the gas flows in consecutive zones of the reaction space. This effect to a certain degree limits the ozone decomposition.

Experimental

Experiments were carried out in the set-up presented on Fig. 2. The ozonizer was thermostated with water (0, 25 and 50°C). The oxygen flow rate (10, 20 and 40 Ndm^3/h) was fixed with the flow controller. Ozone concentration was measured with a BMT-963 VENT ozone-meter.

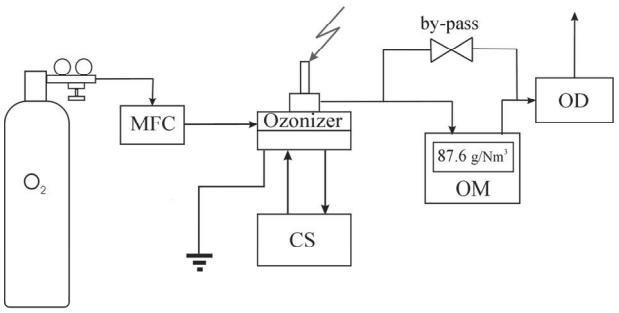

Fig.2. Experimental set-up; MFC – mass flow controller, CS – cooling system, OM – ozone-meter, OD – ozone destructor

Ozonizer and Actuator

Fig. 3 depicts the ozonizer cross-section. Inside the ozonizer the ceramic discharge element (actuator, Fig. 4) was placed. The gas flows towards the middle of the actuator. The actuator was made of an alumina plate with a diameter of 100 mm and a thickness of 1 mm. The ceramic material exhibited a high ozone resistance, a significant electric strength and a stable permittivity over a wide frequency range (ε = 9.1 up to 1 MHz; measured with HP4284A precision LCR meter equipped with HP16451B dielectric test fixture). The thickness of the plate facilitated the heat transfer from the reaction space. On the operating

side of the plate, the electrode consists of concentric strips, which are connected together. The strips on the electrode are 1 mm thick. The distances between them are 2 mm thick. The voltage was applied to the central area of the plate. On the reverse side, an induced electrode was made in the form of a circle with a 90 mm diameter. The electrodes were obtained by 8-10 consecutive depositions of aluminum through a mask. The induced electrode was grounded by the metal wall of the cooling chamber.

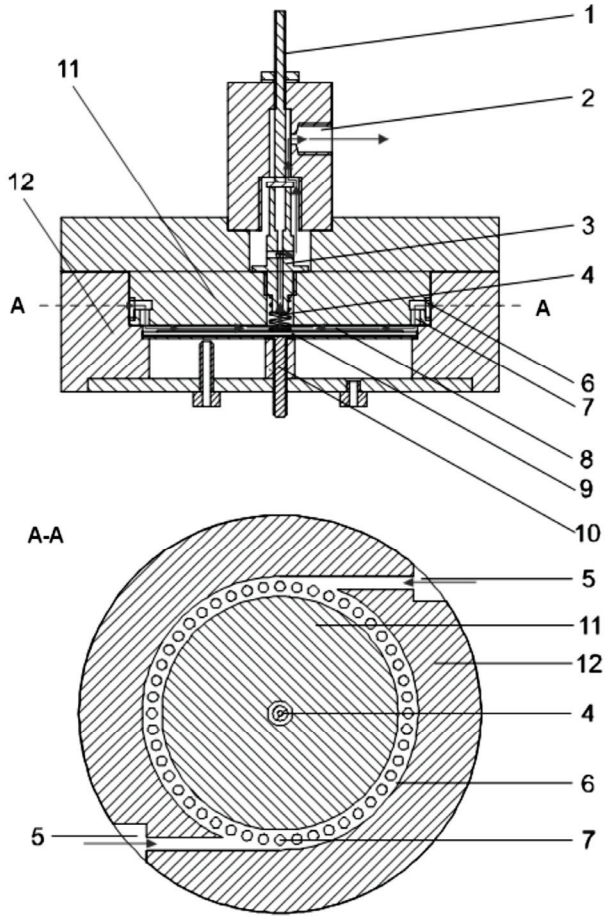

Fig.3. Schematic structure of the ozonizer. In the A-A cross-section the collecting ring with openings can be seen; 1 – high voltage clamp, 2 – outlet of the post-reaction gas, 3 – gas ejector and voltage supply element, 4 – contact spring, 5 – gas inlet channels, 6 – collecting ring, 7 – openings through which the gas enters the reaction space, 8 – reaction space, 9 – actuator, 10 – grounding clamp, 11 – reactor lid, 12 – main body of the reactor.

The ozonizer was supplied with a H.V. push-pull inverter, which generated an alternating current of up to 12 kV_{pp} (ca. 9.2 kHz). The energy consumption was measured with TDS3032 oscilloscope equipped with P6015A and TCP312 probes. Energy efficiency of the ozone synthesis process was calculated on the basis of the formula:

$$\eta \approx c_{O3} \cdot V_0 / P_A, \quad (1)$$

where: η – energy efficiency [g O_3/kWh], c_{O3} – ozone concentration [g O_3/Nm^3], V_0 – gas flow rate [Ndm^3/h], P_A – discharge active power [W].

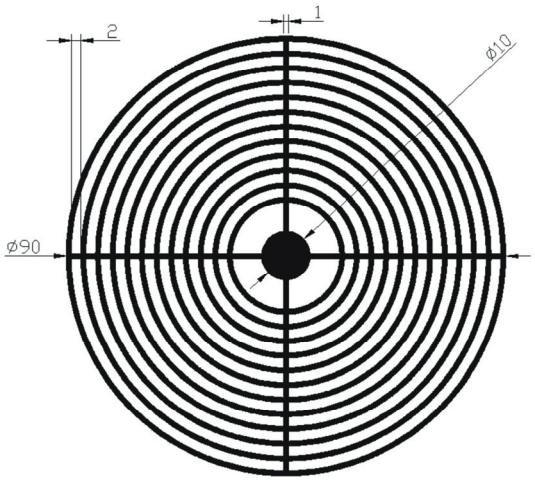

Fig.4. Structure of the strip electrode. Ceramic plate (thickness 1 mm) covered with aluminum coatings (ca. 60 μm)

Results and discussion

Fig. 5 depicts ozone concentrations vs. discharge active power, obtained at the temperatures of 0, 25 and 50ºC and the oxygen flow rate of 10, 20 and 40 Ndm^3/h. The ozone concentrations generally increase when the energy delivered increases, however, the level of the concentrations obtained is diversified. The highest concentration (ca. 125 g/Nm^3) was obtained at the lowest temperature and the lowest oxygen flow rate. The maximum ozone concentration at those conditions was obtained for the active power of ca. 40 W. At 25ºC the maximum concentration (ca. 100 g/Nm^3) was obtained at 30 W. Further increase in power causes a decrease in ozone concentration. An analogous situation appears at 50ºC. The maximum ozone concentration (ca. 85 g/Nm^3) decreases when the power is over ca. 35 W. For the other flow rates the increase of the ozone concentration has a similar character, although the maximum concentrations not always were obtained in the active power examined range.

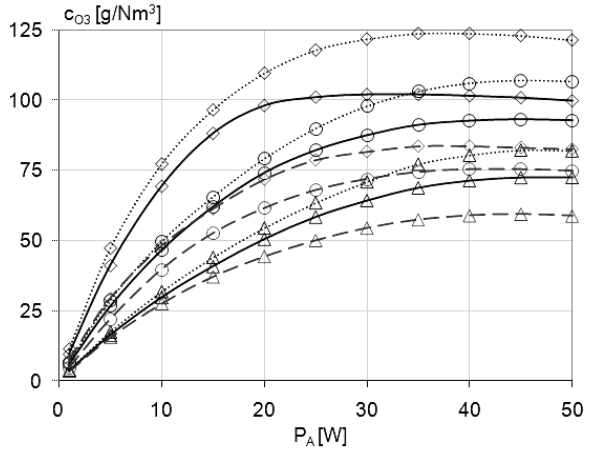

Fig.5. Ozone concentration as a function of active power; oxygen flow rate: ◊ – 10 Ndm^3/h ○ – 20 Ndm^3/h, Δ – 40 Ndm^3/h; temperatures: 0ºC (dot line), 25ºC (solid line), 50ºC (dashed line); frequency 9.2 kHz

It is worth to notice the characteristic shape of the $c(P_A)$ lines obtained at the 10 Ndm^3/h flow rate. At temperatures 0 and 25ºC, ozone concentrations in the range of power lower than 20 W are similar and the considerable difference appears at higher powers. At 50ºC the ozone concentration is considerably lower even at the low power range. It shows the effect of the temperature in the reaction space on the

course of ozone synthesis process. The gas temperature in the reaction space depends on the temperature of cooling liquid, heat transfer conditions and the energy delivered into the system. Only a small part of that energy is consumed for ozone synthesis. The main part of the energy is converted into heat, and increases the gas temperature in the reaction space. The increase of temperature in the system favours the ozone decomposition in accordance with the reaction (R3) of the mechanism of ozone synthesis:

$$O_2 + e \rightarrow O + O + e \qquad k_1 = 2.7\cdot10^{-9} \qquad (R1)$$

$$O_2 + e \rightarrow O(^3P) + O(^3P) + e \qquad (6\ eV) \qquad (R1a)$$

$$O_2 + e \rightarrow O(^1D) + O(^3P) + e \qquad (8{,}4\ eV) \qquad (R1b)$$

$$O + O_2 + M \rightarrow O_3 + M \qquad k_2 = 6.4\cdot10^{-35}\cdot\exp(663/T) \qquad (R2)$$

$$O_3 + O \rightarrow O_2 + O_2 \qquad k_3 = 1.8\cdot10^{-11}\cdot\exp(-2300/T) \qquad (R3)$$

$$O_3 + e \rightarrow O + O_2 + e \qquad k_4 = 3\cdot k_1 \qquad (R4)$$

$$O + O + M \rightarrow O_2 + M \qquad k_5 = (3.8\cdot10^{-30}/T)\cdot\exp(-170/T) \qquad (R5)$$

where M is the third collision partner (O, O_2 or O_3). (All reaction rate constants in: ($cm^3\cdot s^{-1}$) for two bodies collision, ($cm^6\cdot s^{-1}$) for three bodies collision).

Therefore, when the temperature of the cooling liquid is high, unfavourable conditions for the ozone synthesis appear already at low powers of the discharge. Moreover, for small gas flow rate (10 Ndm^3/h), the effectiveness of the convective heat-transfer into the reactor walls is negligibly low. The disadvantageous effect of the cooling liquid temperature appears also for the flow rate of 20 Ndm^3/h (Fig. 5). At the flow rate of 40 Ndm^3/h disadvantageous effect of the high temperature of the cooling liquid (50ºC) is less evident. This effect consistently appears over whole discharge power range. Actually, the ozone synthesis process (and its decomposition) occurs at temperatures higher than the gas temperature. The process occurs in the discharge channels, in which the temperature T (see: reactions R2, R3, and R5) during the short time after the decay of the electrons passage is several dozen degrees higher. As a result the rate of the reaction (R3) increases by ca. 4 % per every temperature-rise degree above the average temperature of the gas.

Energy Efficiency

Fig. 6 depicts the relation between obtained the ozone concentration and the energy efficiency of the process. The highest energy efficiencies were obtained for the lowest ozone concentrations, i.e. at the lowest power (see: Fig. 5). For all temperatures and the gas flow rates energy efficiencies successively decreases. The highest decrease occurs in the range of the highest ozone concentrations, i.e. at the high discharge powers. The highest efficiencies were obtained at the flow rate of 40 Ndm^3/h. At these conditions the high ozone yield was obtained: ca. 2.5 g/h at 50ºC and ca. 3.3 g/h at 0ºC. These results are considerably better than that obtained in tube-type DBD ozonizer, when a double cooled discharge gap was used [11,12]. Both ozonizers were operated at the same temperatures and similar flow rates and active power ranges. However, a completely reliable comparison between both types of discharge is not possible. The experiments were carried out not only in different discharge conditions, but also in ozonizers, whose construction differs. The measurements were conduct at different, both supplying voltages and frequencies. In spite of those differences, the advantages of the presented SD ozonizer are unquestionable. At the same temperatures and comparable flow rates the ozone production is threefold higher, despite a threefold lower cooling surface area. It can not be unequivocally stated, which parameter influences such an advantageous effect on the course of the process at the presence stage of studies. It seems probable that the gas flow rate character (with the systematically increasing linear velocity) has an essential meaning. It should improve the heat transfer between the gas and the dielectric surface. An independent reason could be the lower voltages applied and the faster increase of the electric field strength. As a result, the electrons attain energies sufficient to dissociate the particles of oxygen (6 eV, reaction R1a). If the participation of the electrons with energies considerably exceeding 6 eV were low, the oxygen dissociation in the reaction (R1b) should be limited. As a result the lower part of energy delivered should be changed into heat. The next reason, which could cause an increase in the energy efficiency, is probably the intensive gas mixing. In the literature, the effect of changing the gas velocity in the actuators' strips surrounding is widely reported [5,9,13-16]. These questions are the subject of the current studies.

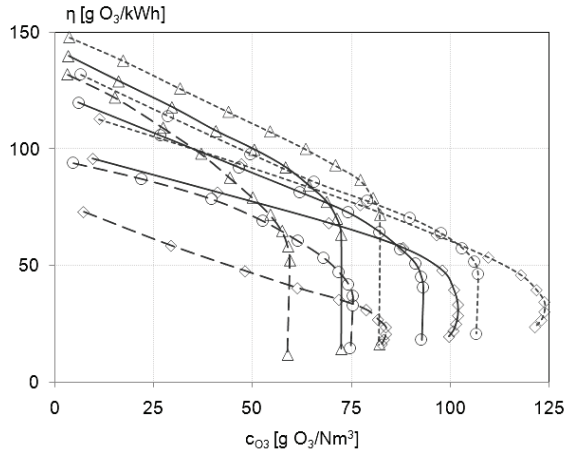

Fig.6. Energy efficiency as a function of ozone concentration; oxygen flow rate: ◊ – 10 Ndm^3/h ○ – 20 Ndm^3/h, Δ – 40 Ndm^3/h; temperatures: 0°C (dot line), 25°C (solid line), 50°C (dashed line); frequency 9.2 kHz

Electric Model of Discharge System

The actuator is a specific capacitor, whose capacity depends on the supplying voltage. When the voltage is low, the capacity depends only on the dimensions of the strips and the thickness of the ceramic plate. At higher voltages, when the discharges proceed on the dielectric surface, the capacity increases, because the active area of the discharge near the strips acts as the additional electrode. his virtual electrode causes the passage of a higher instantaneous current. Fig. 7 depicts the currents in the load. The reactive component I_C of the total current has a regular sine shape. The intensity of the surface current component I_{SD} strongly depends on the polarization of the voltage. At both polarizations, the current passages while the supplying voltage increases (the voltage curve is not presented). At the maximum voltage the discharges decay. The high current passing in the actuator circuit results from the relatively high through capacity between the electrodes (150 pF). The actuator capacity can be reduced for instance by an increase in thickness of the dielectric or changing the induced electrode shape (by decreasing the area of direct interaction of the electrodes). However, it will be connected with worsening of heat transfer conditions. The large surface area of the induced electrode ensures a proper contact with the cooling chamber wall, which is necessary for the carrying away of heat from the reaction space.

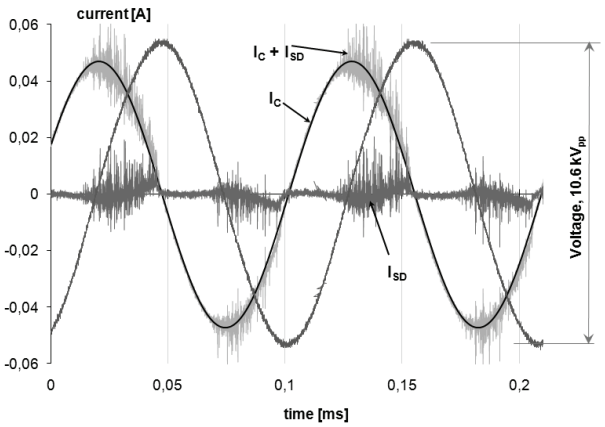

Fig.7. Currents in the high voltage circuit; I_c – capacity current (sine), I_{SD} – surface current; Supplying voltage 10.6 kV_{pp}, frequency 9.2 kHz

Fig. 8 depicts the equivalent circuit diagram of the surface discharge, which is similar to those presented in Fig. 1. However, the current passages by the two arms. The high reactive current continuously passages through the main capacity of the actuator (C_d). When the gas electric strength exceeds, the surface discharge current starts to passage through the capacity C_s. The effect of energy consumption (both, on the ozone synthesis and the gas heating) is represented as the resistance R_s.

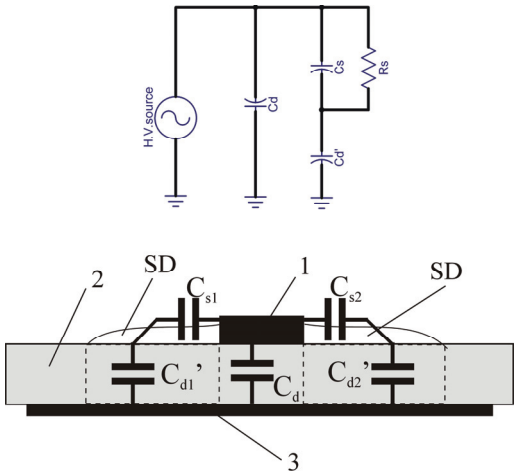

Fig.8. Equivalent circuit diagram of the SD system; Cs – surface capacity, Rs – losses in the surface discharge, Cd – through the solid dielectric capacity (under the strips), Cd' – through the solid dielectric capacity (under the virtual electrode); 1 – high voltage electrode, 2 – dielectric, 3 – induced electrode.

Summary

The circular ozonizer equipped with the flat concentric actuator operating under SD conditions enables to obtain high ozone concentrations. Quite low energy efficiencies of the process result from the usage of single-side cooling of the actuator. However, the SD-type ozonizer with a small electrode surface area enables to obtain a significant ozone yield. The ozone production obtained at 25ºC was only slightly smaller than that at 0ºC, especially at moderate discharge powers.

Because the discharge system was cooled only at the dielectric side, the concentrations of ozone could be probably increased, when cooling the discharge space also at the discharge electrode side.

This study was financially supported by the Ministry of Science and Higher Education from Research Program (2006-2009); Nr. MNiSW N205 012 31/0628.

REFERENCES

[1] Masuda S., Akutsu K., Kuroda M., Awatsu Y., Shiuya Y., A ceramic-based ozonizer using high-frequency discharge, *IEEE Trans. Ind. Appl.*, 34 (1988) No. 2, 223-231
[2] Korzec D., Finantu-Dinu E.G., Dinu G.L., Engemann J., Stefecka M., Kando M., Comparison of planar and surface barrier discharges operated in oxygen-nitrogen gas mixtures, *Surf. & Coat. Techn.*, 174-175 (2003), 503-508
[3] Chen Z., PSpice simulation of one atmosphere uniform glow discharge plasma (OAUGDP) reactor systems, *IEEE Trans. Plasma Science*, 31 (2003) No. 4, 511-520
[4] Opaits D.F., Shneider M.N., Miles R.B., Likhanskii A.V., Macheret S.O., Surface charge in dielectric barrier discharge plasma actuators, *Phys. Plasmas*, 15 (2008), 073505-1-5
[5] Moreau E., Airflows control by non-thermal plasma actuators, *J. Phys D: Appl. Phys.,* 40 (2007), 605-636
[6] Sokolova N.V., Krivov S.A., Volume-surface discharge as an ion source for plasma technologies, *J. Adv. Oxid.Technol.*, 9 (2006) No. 2, 164-169
[7] Williamson J.M., Trump D.D., Bletzinger P., Ganguly B.N., Comparison of high-voltage ac and pulsed operation of a surface dielectric barrier discharge, *J.Phys. D: Appl. Phys.,* 39 (2006), 4400-4406
[8] Humpert C., Pietsch G.J., Simulation of ozone synthesis in oxygen- and air-fed surface discharge arrangements, *Ozone Sci. & Eng.*, 27 (2005), 59-68
[9] Louste C., Artana G., Moreau E., Touchard G., Sliding discharge in air at atmospheric pressure: electrical properties, *J. Electrostat.*, 63 (2005), 615-620
[10] Jodzis S., Kowalska A., Ozone synthesis under pulse discharge conditions, *Prz. Elektrotechniczn (Electrical Review)*, 85 (2009) No. 5, 118-121
[11] Jodzis S., Effect of silica packing on ozone synthesis from oxygen-nitrogen mixtures*, Ozone Sci. & Eng.*, 25 (2003), 63-72
[12] Schmidt-Szałowski K., Jodzis S., Krawczyk K., Młotek M., Górska A., Non-equilibrium plasma process in heterogeneous systems at atmospheric pressure, *Research Trends, Current Topics in Catalysis*, 5 (2006), 39-68
[13] Roth J.R., Aerodynamic flow acceleration using paraelectric and peristaltic electrohydrodynamic effects of a One Atmosphere Uniform Glow Discharge Plasma*, Physics of Plasma,* 10 (2003), Nr. 5, 2117-2126
[14] Dong B., Bauchire J.M., Pouvesle J.M., Magnier P., Hong D., Experimental study of a DBD surface discharge for the active control of subsonic airflow*, J. Phys. D: Appl. Phys.,* 41 (2008), 155201 (9pp)
[15] Podliński J., Berendt A., Mizeraczyk J., Elongated DBD with floating electrodes for actuators, *12th Int. Symp. on High Pressure Low Temperature Plasma Chemistry, Trenčianske Teplice, Slovakia, 12-17 Sept., Book of Contributed Papers,* Vol. 1 (2010), 74-78
[16] Pavon S., Dorier J.-L., Hollenstein Ch., Ott P., Leyland P., Effects of high-speed airflows on a surface dielectric barrier discharge, *J. Phys. D: Appl. Phys.,* 40 (2007), 1773–1741

***Authors**: dr inż. Sławomir Jodzis, Politechnika Warszawska, Wydział Chemiczny, ul. Noakowskiego 3, 00-664 Warszawa, E-mail: jodzis@ch.pw.edu.pl*